1 **Mapping mining-affected water pollution in China: Status, patterns, risks, and**

2 **implications**

4 Ziyue Yin[1], Jian Song[2], Dianguang Liu[1], Jianfeng Wu[1,*], Yun Yang[2], Yuanyuan Sun[1], Jichun Wu[1]

6 [1] Key Laboratory of Surficial Geochemistry, Ministry of Education, Department of Hydrosciences,

7 School of Earth Sciences and Engineering, Nanjing University, Nanjing 210023, China

8 [2] School of Earth Sciences and Engineering, Hohai University, Nanjing 211100, China

11 [*] Corresponding authors. Tel: +86 25 89680853; fax: +86 25 83686016

12 *E-mail address*: jfwu@nju.edu.cn (J.F. Wu)

Abstract: Mining-affected water pollution poses a serious threat to human health and economic prosperity globally. The human toxicity and ecosystem impacts induced by mining activities have achieved considerable public, scientific, and regulatory attention. In this study, a comprehensive database of 8,433 water samples from 211 coal mines and 87 metal mines in China was established to reveal the national status and spatial heterogeneity of mining-affected water pollution, human health risks, and their potential multifaceted challenges. The results show that the concentrations of sulfate, Fe, Mn, Al, and several heavy metals in the mining-affected water of metal mines are generally higher than those of coal mines, especially in acid water (pH < 6.5). In terms of spatial distribution, the gridded data demonstrates that the southern regions in China, especially Guizhou, Guangdong, Fujian, Jiangxi, Hunan, and Guangxi provinces/autonomous regions, are the hotspots of mining-affected water pollution (*i.e.*, low pH as well as high sulfate, Fe, Mn, and heavy metals). The unacceptable carcinogenic risks caused by poor-quality surface water and groundwater are observed in 51.52% (for adults) and 29.29% (for children) of the mining areas. Moreover, severe non-carcinogenic risks are also identified in 68.07% and 80.67% of mining areas for adults and children, respectively. Overall, the acid and metal-rich water exhibits a widespread and detrimental impact in China, especially in the southern regions, posing significant risks to planetary health by degrading surface water and groundwater quality, destroying biodiversity, and threatening human well-being. This study provides a thorough set of scientific data on surface water and groundwater quality in mining areas to guide policymakers in designing differentiated management strategies for the sustainable development of coal and metal mines.

Keywords: Mining-affected water pollution; Spatial patterns; Risk assessment; Adverse effects; Differentiated management.

1 Introduction

Coal and metalliferous mineral resources are essential materials for global socio-economic development. The extraction and processing of minerals have caused detrimental impacts on aquatic ecosystems, soil ecosystems, living organisms, and human health worldwide (Blowes et al., 2014; Li et al., 2014; Havig et al., 2017; Ighalo et al., 2022). Mine drainage and leachate from active and abandoned mines are of global concern as they continue to release harmful substances into the underlying geological materials or adjacent water bodies for decades, inevitably leading to the degradation of both surface water and groundwater quality (Acharya and Kharel, 2020; Ighalo and Adeniyi, 2020). In particular, the environmental risks induced by acid mine drainage (AMD) have been ranked second only to global warming and ozone depletion (Moodley et al., 2018; Ai et al., 2023). Mining-affected water is generally characterized as metalliferous. Certain metals, such as Cu, Fe, Mn, and Zn, function as essential trace elements in human physiological processes. However, when their concentrations exceed specific thresholds in surface water and groundwater systems, these biologically relevant metals can pose significant toxicological risks to ecosystems and human health (Wei et al., 2022). Other non-essential heavy metals (HMs), including As, Cd, Cr, Hg, Ni, and Pb, have no nutritional or beneficial effects on humans. They can be toxic even at low concentrations and are therefore recognized as carcinogenic, mutagenic, and teratogenic. In addition, the persistence, toxicity, mobility, and non-biodegradability of HMs potentially form an enduring environmental footprint that jeopardizes ecosystems (He et al., 2013; Dippong et al., 2024). Consequently, there is a growing demand in mining areas for assessing the status of pollution and associated risks, as well as developing more effective management strategies and policies to mitigate these detrimental impacts (Cheng 2003; Hu et al., 2014).

Exploring the heterogeneity, risks, and threats of mining-affected water pollution is desirable but remains challenging. More recently, an increasing number of studies have been focused on the mining-affected water pollution from coal mines in major coal-producing countries (Sun et al., 2013; 2020; 2025; Acharya and Kharel, 2020; Dong et al., 2022; Ai et al., 2023; Hou et al., 2024; Kumar et al., 2024). For instance, Acharya and Kharel (2020) provided an in-depth overview of the formation and effects of AMD from coal mining in the United States, reviewed prediction and treatment methods, identified key research gaps, and explored the challenges and opportunities that AMD posed for scientists and researchers. Ai et al. (2023) developed a conceptual model to illustrate the formation and evolution of AMD in the coal mines from a life-cycle perspective. Meanwhile, the critical governing factors and treatment technologies of AMD across abandoned mines in major coal-producing countries were identified, including China, the United States, the United Kingdom, Australia, and India. Coal and metal mines have different priority pollutants and levels of pollution due to differences in geological conditions and mineral extraction methods (Yu et al., 2024). Comparative studies of the status, heterogeneity, risks, and impacts of water pollution in coal and metal mines achieved limited concerns so far. It is essential for the development of remediation strategies and the implementation of risk-based, differentiated management practices to achieve sustainability in mining areas associated with the mineral economy.

To our knowledge, previous studies have provided a solid basis for the soil pollution status of HMs and their related health risk at the national or global scale (Li et al., 2014; Liu et al., 2020; Hou et al., 2023; Shi et al., 2023). For example, Shi et al. (2023) identified the spatiotemporal distribution of soil HM concentrations based on studies conducted between 1977 and 2020. In addition, the ecological and human health risks were assessed concerning different land use types

at the national scale. Yu et al. (2024) provided a more comprehensive analysis of the pollution characteristics, spatial distribution, major influencing factors, and probabilistic health risks of potentially toxic elements in soil, using data from 110 coal mines and 168 metal mines across China. However, systematic studies of water pollution status and risks have yet to be undertaken at a national or even broader scale, as current research only focused on water pollution and risks in specific mining areas (He et al., 1998; Xiao et al., 2003; Wang et al., 2019; Chen et al., 2020; Wang et al., 2023). Therefore, it is necessary to implement deep mining of massive hydrochemical data and establish a nationwide database that can identify the spatial pattern of mining-affected water pollution and support risk assessment.

China, the second-largest economy worldwide, has various and extensive mineral resources (Li et al., 2014). It has been demonstrated that there are 171 types of mineral resources in China, with proven reserves accounting for 12% of the world's mineral resources (Hu et al., 2009). Furthermore, China is one of the largest global producers and consumers of metals and metalloids, such as Fe, Mn, Zn, Pb, Sb, and Sn (Gunson and Jian, 2001). China's coal reserves of 143,197 million tons (Mt) rank fourth globally, while its annual production of 2,971 Mt leads worldwide (Blowes et al., 2014; Ai et al., 2023). The coal extraction inevitably generates substantial amounts of mine water, resulting in a series of water environmental issues (Zhang et al., 2016b; Qu et al., 2023). For example, Gu et al. (2021) demonstrated a 2:1 mine water to coal production ratio, with approximately 2 tons of mine water produced per ton of extracted coal in China. In recent years, China has put forward a series of monitoring, prevention, management, and remediation measures to improve water quality and ensure water supply safety. However, the detrimental impacts triggered by mining activities on the aquatic environment have not been well managed. Since 2010,

101   China has implemented a policy-driven initiative to phase out nearly 12,000 coal mines to address

102   two critical challenges, *i.e.*, the declining economic viability and the escalating environmental

103   externalities (Ma et al., 2020). These policies effectively restore water storage capacity in mining

104   regions. However, sulfates and dissolved metals generated by complex geochemical processes

105   during the weathering of sulfide minerals may migrate and transform within the recovering

106   groundwater system, thereby increasing the ecological vulnerability of local hydrological networks.

107   Therefore, the objectives of the study are: (i) to establish a national-scale high-quality database

108   containing basic water quality information for typical coal and metal mines; (ii) to reveal spatial

109   heterogeneity of mining-affected water and evaluate health risks posed by potentially toxic

110   elements from coal and metal mines drainage in China; and (iii) to highlight the negative impacts

111   and discuss the management implications in the differentiated policy for different mine types (coal

112   or metal) and multiple mining phases (active or abandoned). Exploring the spatial heterogeneity of

113   mining-affected water in China is of great importance to achieve deep insights for designing the

114   targeted and promising mitigation strategies at the different spatial scales, which is critical to

115   implementing the optimal trade-offs between green mining and human health.

116   **2   Data and methodology**

117   *2.1   Data mining and processing*

118   The belief information of natural resources in China has been presented in Section S1 of the

119   Supplement, which serves as the cornerstone for the database development, spatial pattern analysis,

120   and risk assessment in the study. Specifically, Figs. S1 and S2 illustrate the spatial distribution and

121   total sulfur content of coal-bearing areas in China, and Fig. S3 exhibits the spatial distribution of

122   the major non-ferrous mineral resources in China. In this study, the composite database integrates

123   mining-affected water (surface water and groundwater) quality parameters systematically extracted

124   from 293 peer-reviewed studies published over the past decades. The primary data were obtained

125   from mainstream online bibliographic databases, such as China National Knowledge Infrastructure,

126   China Wanfang Literature Database, Web of Science, Elsevier, Springer, Wiley, Taylor & Francis,

127   and the Multidisciplinary Digital Publishing Institute. The screening keywords were 'China', 'coal

128   mine', 'metal mine', 'acid mine drainage', 'mine water', 'surface water', 'groundwater',

129   'hydrochemistry', and 'heavy metals'. All retrieved literature was downloaded by 2024/4/25, and

130   the irrelevant studies were eliminated based on their abstracts, data, and full-text content.

131   *2.2   Quality assessment*

132   To ensure the reliability of the data, the collected literature was assessed for quality based on

133   the following criteria: (i) adhering to strict quality assurance/quality control procedures during

134   sampling, storage, and laboratory testing to ensure consistency, precision, and accuracy of results;

135   (ii) extracting the sampling year (if not stated, the received or published date of the manuscript was

136   adopted); (iii) extracting the latitude and longitude coordinates of the sampling site, mine or the

137   county-level city in which they are located; and (iv) extracting the concentration of the featured

138   component or statistics (minimum, mean and maximum value) based on the original data.

139   *2.3   Database establishment*

140   To assess the national extent of mining-affected water pollution, a comprehensive database of

141   8,433 data (6,175 coal mine data and 2,258 metal mine data) derived from 298 mines was

142   established, including 211 coal mines and 87 metal mines (*i.e.*, antimony mine, copper mine, gold

143   mine, hematite mine, iron mine, lead-zinc mine, molybdenum mine, polymetallic mine, pyrite mine,

144   rare earth mine, thallium-mercury mine, tin mine, tungsten mine, and uranium mine). The spatial

145   distribution of the sampling site used in the study and the data classification at the provincial level

146   are displayed in Fig. 1. The detailed information includes the sample ID, province, county/mine

147   name, latitude (N), longitude (E), mine type, mine status (active or abandoned), sampling year,

148   sampling month, sample type, basic physiochemical characteristics (pH, temperature (T), electrical

149   conductivity (EC), oxidation reduction potential (ORP), dissolved oxygen (DO), and total

150   dissolved solids (TDS)), major cation/anion ions (Na^+, K^+, Ca^{2+}, Mg^{2+}, Cl^-, SO_4^{2-}, HCO_3^-, NO_3^- and

151   F^-), Fe, Mn, Al, HMs (Cr, Ni, Cu, Zn, As, Cd, Hg, and Pb) and data source. The typical mine lists

152   used in the study are shown in Table S1.
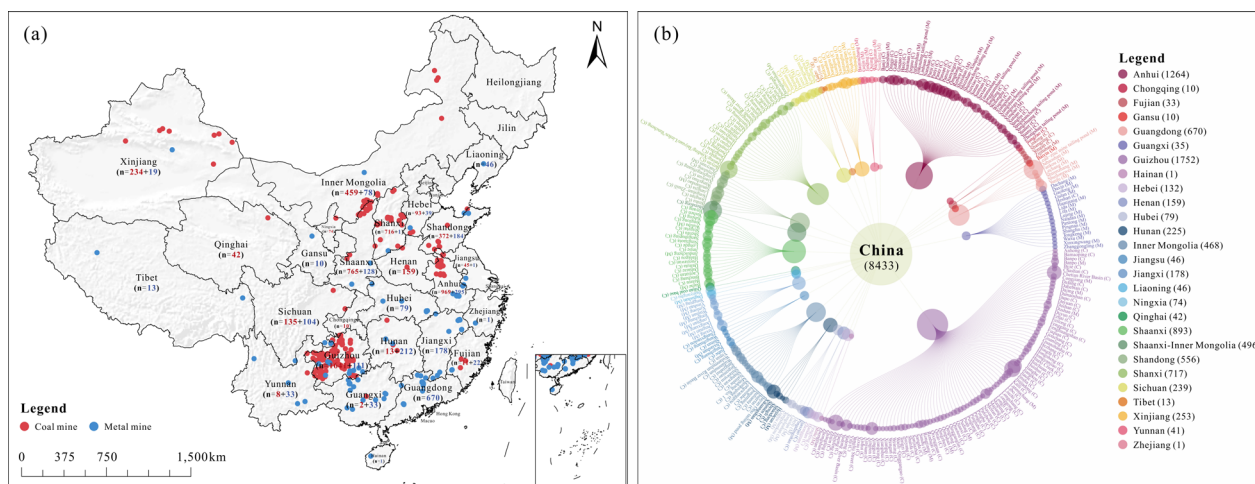
154   **Figure 1.** The information on data sources for this study, including (a) the spatial distribution of

155   the sampling site, and (b) the data classification at the provincial level. In Fig. 1a, the value in the

156   bracket represents the sample size (n), specially, the red and blue numbers are the sample sizes of

157   coal mines and metal mines for different provinces, respectively. In Fig. 1b, the size of the inner

158   circle represents the sample size at the provincial level, while the size of the outer circle represents

159   the sample size at the specific mine level (the letters 'C' and 'M' in the brackets represent coal mine

160   and metal mine, respectively). In the legend, the value in the bracket represents the sample size of

161   the different provinces.

162   *2.4 Risk assessment*

163   Human exposure to metals can occur through various pathways, including ingestion and

164   dermal contact with contaminated water. Therefore, these two pathways are considered to assess

165   the potential human risks, *i.e*., non-carcinogenic risks (NCRs) and carcinogenic risks (CRs), for

166   adults and children. The model developed by the U.S. Environmental Protection Agency (US EPA)

167   is employed for risk assessment in this study (US EPA, 2004; 2011):

168
$$ADI_{ing} = \frac{C_w \times IR \times EF \times ED}{BW \times AT} \tag{1}$$

169
$$ADI_{der} = \frac{C_w \times K_p \times ET \times SA \times EF \times ED \times CF}{BW \times AT} \tag{2}$$

170   where ADI_{ing} and ADI_{der} are the average daily intake by ingestion and dermal adsorption (mg/kg·d),

171   respectively; C_w is the metal concentration in the mining-affected water (mg/L); IR is the ingestion

172   rate (L/d); EF is the exposure frequency (d/yr); ED is the exposure duration (yr); K_p is the

173   permeability coefficient of skin (cm/h); ET is the exposure time (h/d); SA is the exposed skin

174   surface area (cm^2); CF is the conversion factor (L/cm^3), which is set to 0.001 in the study; BW is

175   the body weight (kg); and AT is the averaging time (d).

176   The hazard quotient (HQ) and hazard index (HI) are used to determine the NCRs to human

177   health (Dippong et al., 2024). The HQ to residents (adults and children) from metal exposure via

178   ingestion (HQ_{ing}) and dermal absorption (HQ_{der}) are quantified:

179
$$HQ_{ing} = \frac{ADI_{ing}}{RfD_o} \quad \text{and} \quad HQ_{der} = \frac{ADI_{der}}{RfD_{der}} \tag{3}$$

$$180 \qquad HI = \sum HQ_i = HQ_{ing} + HQ_{der} \qquad\qquad (4)$$

181   where HI is the hazard index, which is the sum of HQ. HI > 1 indicates potential adverse effects

182   on human health, whereas HI < 1 suggests no NCR is present; RfD_o is the reference dose for oral

183   intake; and RfD_{der} is the reference dose for dermal exposure, which can be calculated by:

$$184 \qquad RfD_{der} = RfD_o \times ABS_{GI} \qquad\qquad (5)$$

185   where ABS_{GI} is the gastrointestinal digestion coefficient (unitless).

186   The CRs to residents from ingestion and dermal absorption of mining-affected water are

187   determined using Eqs. (6) and (7):

$$188 \qquad CR_{ing} = ADI_{ing} \times SF \quad and \quad CR_{der} = ADI_{der} \times SF \qquad\qquad (6)$$

$$189 \qquad TCR = \sum CR_i = CR_{ing} + CR_{der} \qquad\qquad (7)$$

190   where TCR is the total CR, if TCR > 10^{-4}, there is a significant risk to humans, and if $10^{-6} \leq$ TCR

191    $\leq 10^{-4}$, the risk is generally acceptable; CR_{ing} and CR_{der} are the CRs induced by ingestion and dermal

192   contact with mining-affected water, respectively; SF is the slope factor. The detailed values of the

193   parameters in the above formula (Eqs. (1) - (7)) are represented in Tables S2 and S3.

194   **3   Results and analysis**

195   *3.1   Overview of mining-affected water in China*

196   All the data were collected from 26 provinces in China, while Beijing, Tianjin, Shanghai,

197   Heilongjiang, Jilin, Hong Kong, Macao, and Taiwan did not meet the data extraction principles. At

198   the provincial administrative level, five regions (*i.e.*, Guizhou, Anhui, Shaanxi, Shanxi, and

199   Guangdong) have a statistically significant representation in sample collection. Among these,

200   Guizhou and Anhui exhibit the most substantial data size, accounting for 20.78% and 14.99% of

201 the total national dataset, respectively (Fig. 1). The spatial distribution of the sample size for each

202 component at the 0.5° grid scale is depicted in Fig. S4. In general, most of the data show the basic

203 information of the water sample, such as pH value and the concentrations of major cation and anion

204 ions. In addition, many studies focused on the status of HM pollution in the mining areas, with a

205 multi-source research synthesis revealing substantial monitoring coverage of 2,241 (Fe), 2,265

206 (Mn), 1,401 (Al), 952 (Cr), 691 (Ni), 1,563 (Cu), 1,575 (Zn), 1,451 (As), 1,627 (Cd), 280 (Hg),

207 and 1,425 (Pb) water samples nationwide. Therefore, the Fe, Mn, Cd, Cu, and Zn are priority

208 investigative targets for mine water research. The statistics of acid and neutral/alkaline mining-

209 affected water in China are presented in Table 1. The pH and multi-component concentrations of

210 mining-affected water in China are shown in Fig. 2.

211
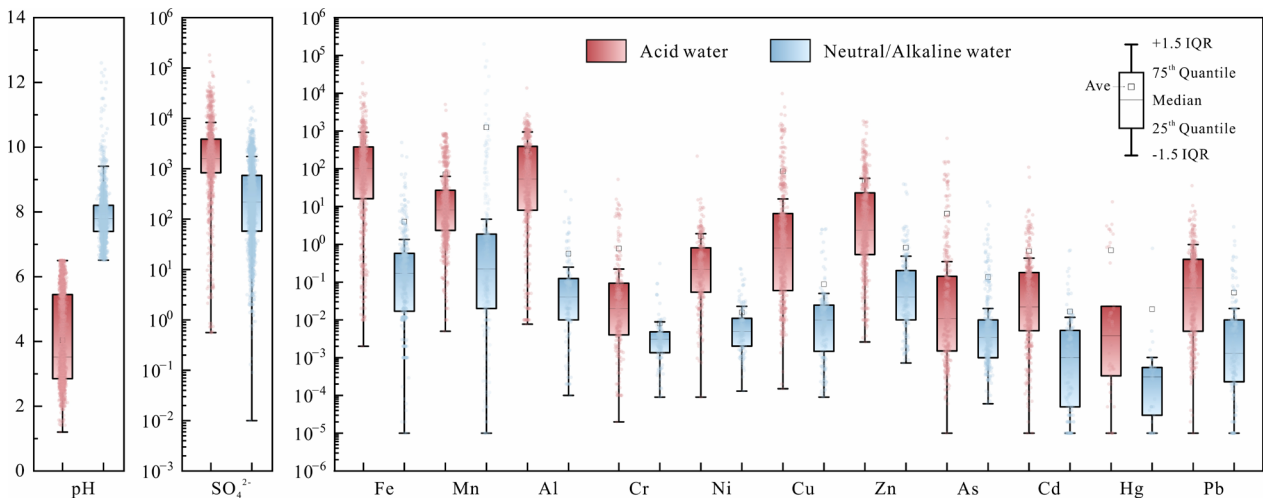
212 **Figure 2.** Boxplots of the pH and multi-component concentrations (mg/L) of mining-affected water

213 in China.

Table 1. The statistics of mining-affected water in China (Units are mg/L except pH).

Item	Acid mining-affected water				Non-acid mining-affected water			
	Min	Median	Ave	Max	Min	Median	Ave	Max
pH	1.20	3.52	4.04	6.50	6.51	7.80	7.85	12.60
Na^+	0.00	15.60	55.39	1613.00	0.23	156.01	403.20	9371.00
K^+	0.00	3.30	6.41	172.00	0.00	3.11	7.10	419.00
Ca^{2+}	0.83	284.80	284.33	987.97	0.00	64.10	119.76	4841.70
Mg^{2+}	0.01	75.33	388.36	10992.00	0.00	19.01	52.85	12752.00
Cl^-	0.00	3. 50	35.50	3097.40	0.00	51.68	314.21	26265.00
SO_4^{2-}	0.56	1580.16	4648.54	181000.00	0.01	181.27	621.24	52915.00
HCO_3^-	0.00	1.89	48.65	769.00	0.00	253.23	343.13	4976.61
NO_3^-	0.00	0.80	16.46	735.60	0.00	3.78	16.02	1774.95
F^-	0.00	0.69	4.17	238.34	0.00	0.81	1.91	100.00
Fe	0.0020	103.3000	520.4396	65250.0000	0.0000	0.1700	3.9788	495.4300
Mn	0.0050	8.1080	71.1849	5050.0000	0.0000	0.2164	1258.9853	200000.0000
Al	0.0077	53.9000	304.9210	13679.0000	0.0001	0.0350	0.5306	25.0000
Cr	0.0000	0.0200	0.7725	52.2700	0.0001	0.0031	0.0081	0.3100
Ni	0.0001	0.2166	1.6396	216.0000	0.0001	0.0050	0.0159	0.2260
Cu	0.0002	0.8010	85.6400	9777.7700	0.0001	0.0100	0.0678	2.5600
Zn	0.0026	2.3685	46.6335	1834.0000	0.0007	0.0391	0.5292	39.3000
As	0.0000	0.0108	6.4969	641.7000	0.0001	0.0034	0.1362	13.0000
Cd	0.0000	0.0220	0.6552	110.0000	0.0000	0.0004	0.0108	0.6677
Hg	0.0000	0.0038	0.6997	13.3600	0.0000	0.0003	0.0196	0.7833
Pb	0.0000	0.0700	0.5090	35.6800	0.0000	0.0012	0.0307	1.2200

215   It should be highlighted that the mean values may result in overestimation, as some extremely

216   high values are observed in the surveyed mines, such as the Baiyin copper mine, Bainiuchang

217   polymetallic mine, Zijinshan copper mine, and so on. Therefore, median values are selected to

218   represent the national characteristics of the mining-affected water pollution in this section. The pH

219   value of acid water (*i.e.*, pH < 6.5) ranges from 1.20 to 6.50, with a median (interquartile range,

220   IQR) of 3.52 (2.85, 5.45) (CV = 34.39%). In comparison, neutral/alkaline water has a pH value

221   between 6.51 and 12.60, with a median of 7.80 (IQR: 7.40, 8.20) (CV = 8.99%). Generally, the

222   SO_4^{2-} concentration of acid water is higher than that of neutral/alkaline water (Figs. 2 and 3). The

223   former ranges from 0.56 to 181000 mg/L (25th percentile = 834.33 mg/L, median = 1580.16 mg/L,

224   75th percentile = 3864.08 mg/L, and CV = 222.70%). And the latter from 0.01 to 52915 mg/L (25th

225   percentile = 52.87 mg/L, median = 181.27 mg/L, 75th percentile = 558.73 mg/L, and CV =

226   264.02%). Furthermore, the results indicate that the detectable medians of the multi-metal

227   concentrations (mg/L) in acid water follow the order: Fe (103.30) > Al (53.90) > Mn (8.1080) > Zn

228   (2.3685) > Cu (0.8010) > Ni (0.2166) > Pb (0.0700) > Cd (0.0220) > Cr (0.0200) > As (0.0108) >

229   Hg (0.0038), while that of the neutral/alkaline water is Mn (0.2164) > Fe (0.1700) > Zn (0.0391) >

230   Al (0.0350) > Cu (0.0100) > Ni (0.0050) > As (0.0034) > Cr (0.0031) > Pb (0.0012) > Cd (0.0004) >

231   Hg (0.0003).

3.1.1 *Contents of acid mining-affected water in China*

233   The multi-component concentrations of mining-affected water in both coal and metal mines

234   are displayed in Figs. 3 and S5, and the statistics are given in detail in Table S4. It is obvious that

235   the concentrations of sulfate, Fe, Mn, Al, and several HMs in the mining-affected water of most

236   metal mines are higher than that of coal mines, especially in mining-affected water with low pH (<

237 6.5). For acid mining-affected water, the pH of coal mines is approximately 1.90 - 6.50 (with a

238 median of 4.50), while the pH of metal mines is approximately 1.20 - 6.50 (with a median of 3.10).

239 The medians (IQR) of SO_4^{2-} are 1381.59 (871.41, 1954.73) mg/L and 2982.00 (778.15, 10200.00)

240 mg/L for coal mines and metal mines, respectively. In conjunction with Fig. S6, it can be seen that

241 the detectable medians of multi-metal concentrations (mg/L) in coal mining-affected water are

242 77.41 (Fe), 12.87 (Al), 3.50 (Mn), 0.4211 (Zn), 0.1796 (Ni), 0.0431 (Cu), 0.0080 (Cr), 0.0036 (Cd),

243 0.0034 (As), 0.0023 (Pb), and 0.0004 (Hg), respectively. Additionally, the detectable medians of

244 multi-metal concentrations (mg/L) in metal mining-affected water are 152.00 (Al), 113.77 (Fe),

245 15.82 (Mn), 7.200 (Zn), 1.7325 (Cu), 0.2142 (Ni), 0.1498 (Pb), 0.0500 (Cr), 0.0383 (Cd), 0.0281

246 (As), and 0.0090 (Hg), respectively.
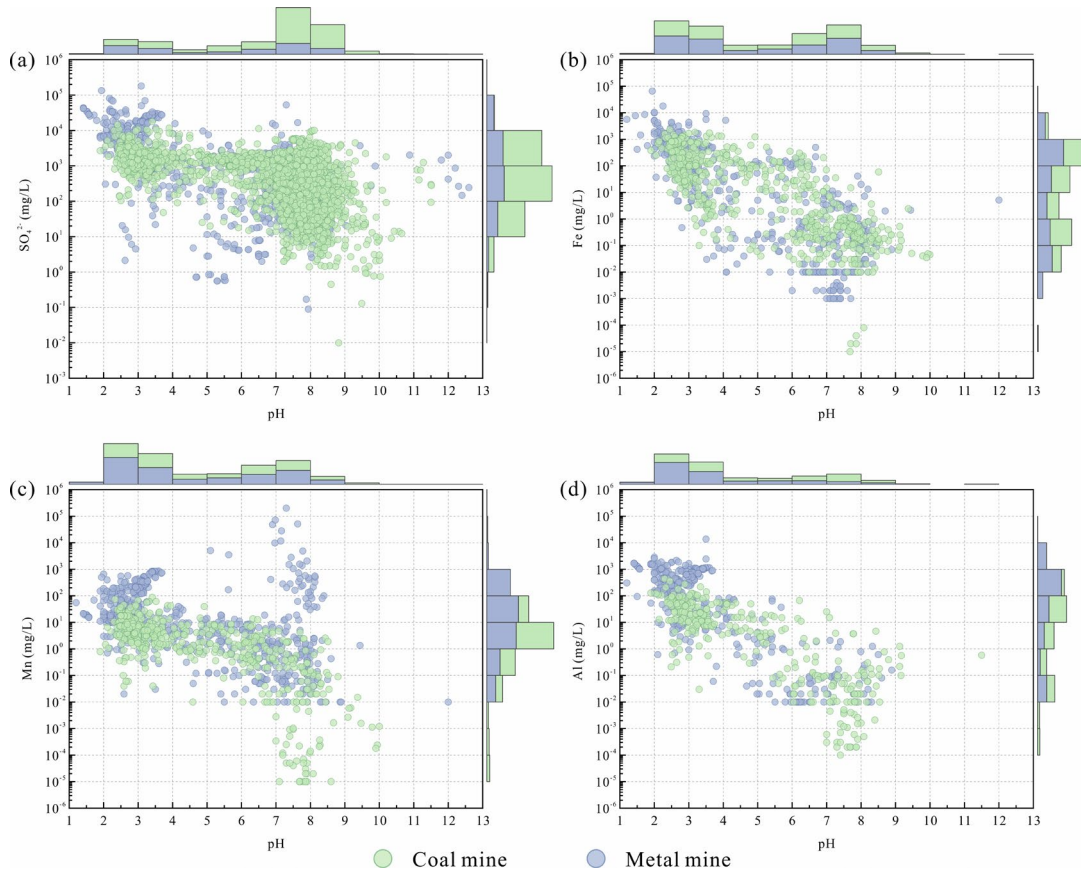
247

248 **Figure 3.** The respective relationship of pH versus (a) SO_4^{2-}, (b) Fe, (c) Mn, and (d) Al in coal and

249 metal mines.

3.1.2 Contents of non-acid mining-affected water

Similarly, for non-acid mining-affected water, the pH value of coal mines is about 6.51 - 11.51 (with a median of 7.82), while that of metal mines is about 6.51 - 12.60 (with a median of 7.70). The medians (IQR) of SO_4^{2-} are 193.51 (48.97, 582.70) mg/L and 157.41 (60.23, 425.33) mg/L for coal mines and metal mines, respectively. As shown in Fig. S6, the results indicate that the detectable medians of multi-metal concentrations (mg/L) in coal mines are in the order of Fe (0.2500) > Mn (0.0204) > Al (0.0200) > Zn (0.0048) > Ni (0.0040) > Cr (0.0022) > As (0.0016) > Cu (0.0010) > Pb (0.0003) > Hg (0.0001) > Cd (0.0000), respectively. The detectable median concentrations (mg/L) of Mn, Zn, Al, Fe, Cu, Pb, Ni, Cr, As, Cd, and Hg in metal mines are 0.7612, 0.0692, 0.0575, 0.0484, 0.0196, 0.0068, 0.0065, 0.0042, 0.0040, 0.0017, and 0.0003, respectively. In addition, the results of non-parametric tests (*i.e.*, Mann-Whitney U-test and Spearman's rank correlation) are presented in the Section S2 (Fig. S7) of the Supplement.

3.2 Spatial patterns of mining-affected water pollution in China

The coal mines surveyed in the study are mainly located in the northern and southwestern regions, which together account for approximately 70% of the national coal production. This localized distribution aligns closely with the pattern of coal-mining belts in China. The southwestern and southern regions of China, rich in metallic mineral resources and with complex geological conditions, have been subject to frequent or unregulated mining activities for many years. Conversely, the western and northern regions are relatively poorly endowed with metal resources (Yu et al., 2024). The mining-affected water is divided into 4 types in the study based on the multi-component characteristic, *i.e.*, with low pH, with high sulfate, with high Fe and Mn, and

271 with high HMs. Given that mining activities have posed great threats to the surface water and

272 groundwater, the classification thresholds incorporated both the distribution of the collected data

273 and regulatory benchmarks from the Environmental Quality Standards for Surface Water (GB

274 3838-2002) and the Standard for Groundwater Quality (GB/T14848-2017) in China. The categories

275 of water quality in the above documents are listed in Tables S5 and S6. Figs. 4 and S8 showcase

276 the regional patterns of the mining-affected water, and a decreasing trend in pollution levels can be

277 observed from South China to North China.

278
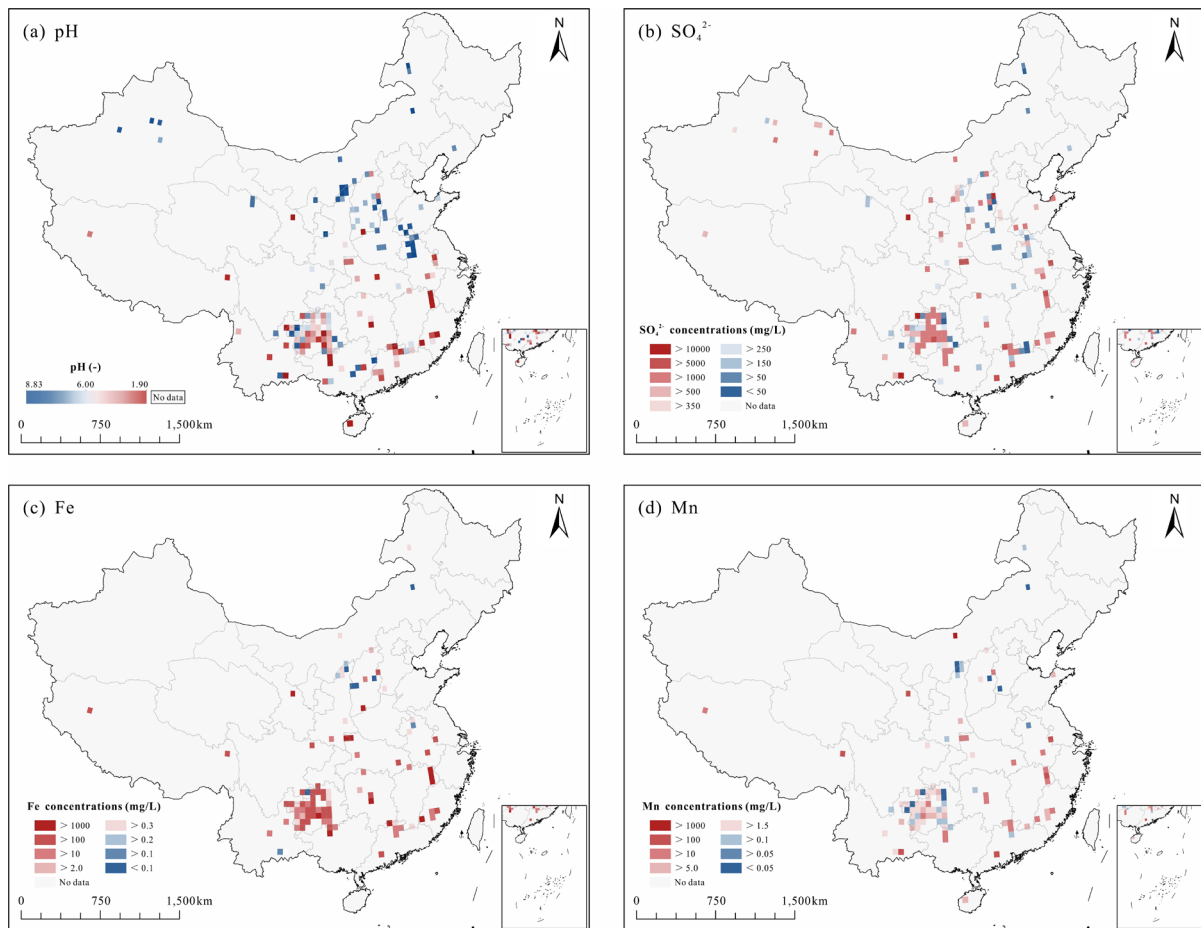
279 **Figure 4.** The spatial distribution of (a) pH; and the mean concentration of individual components

280 (mg/L) showing respective (b) SO_4^{2-}, (c) Fe, and (d) Mn in mining-affected water on the 0.5° grid.

3.2.1 Mining-affected water with low pH

The acid mine water is the predominant contaminant subtype, with pH values significantly below natural freshwater baselines (generally between 2.0 and 4.0). AMD is generally associated with the extraction and processing of sulfur-bearing metalliferous ore deposits (*e.g.*, pyrite, chalcopyrite, pyrrhotite, and sphalerite) and sulfide-rich coal in China (Blowes et al., 2014; Feng et al., 2014). Spatial pattern analysis revealed intense acidification hotspots (pH < 6.5) concentrated in South China, especially in the provinces of Fujian, Guangdong, Guizhou, Hubei, Hunan, Jiangxi, and Yunnan. In particular, the pH of Fuquan City in Guizhou Province reached 1.90, indicating extreme acidity. Combined with the results of the Spearman correlation analysis, a strong geochemical coupling between acidity, sulfate, and dissolved metals can be observed.

3.2.2 Mining-affected water with high sulfate

It is evident that there is a spatial consistency in the distribution of high-sulfate mining-affected water and acid water (Fig. 4b). The quantitative assessment of 138 data grids demonstrates that 73.9% ($n = 102$) exceed the sulfate threshold concentration of 250 mg/L. In addition, the high sulfate mining-affected water pollution is also particularly prevalent in the provinces/autonomous regions of Anhui, Hebei, Shandong, Shaanxi-Inner Mongolia, and Xinjiang, where the pH values are generally > 6.5. Contrary to typical AMD paradigms, there are two pathways to produce non-acid, high-sulfate water in the neutral/alkaline-pH systems: (i) by pyrite oxidation followed by natural neutralization, and (ii) by dissolution of sulfur-bearing and gypsum minerals. For instance, the Ordovician limestone aquifer is composed of dolomite, which is the primary source of sulfate in southwest Shandong (*e.g.*, Hongshan-Zhaili mines), Anhui (*e.g.*, Huainan-Huaibei mines) and

302   other mining areas. The above-mentioned spatial heterogeneities found in our study are in good

303   agreement with the results of Feng et al. (2014).

304   *3.2.3 Mining-affected water with high Fe and Mn*

305   Nationally, dissolved Fe and Mn concentrations far exceed the Class III threshold for

306   groundwater in China (GB/T14848-2017: Fe > 0.3 mg/L, Mn > 0.1 mg/L). Spatial pattern analysis

307   identifies six critical Fe contamination hotspots (Fig. 4c): Fujian (*e.g.*, Zijinshan copper mine),

308   Guangdong (*e.g.*, Lechang lead-zinc mine), Gansu (*e.g.*, Baiyin copper mine), Hunan (*e.g.*,

309   Shaodong coal mine), Jiangxi (*e.g.*, Dexing/Yongping copper mines) and Shannxi (*e.g.*, Baihe

310   pyrite mine) provinces, where the concentrations even exceed 1000 mg/L. Parallel spatial patterns

311   emerge for Mn contamination (Fig. 4d). Guangdong (*e.g.*, Yunfu pyrite mine), Gansu (*e.g.*, Baiyin

312   copper mine), Inner Mongolia (*e.g.*, Bayan Obo pyrite mine), Jiangxi (*e.g.*, Dexing copper mine),

313   Tibet (*e.g.*, Yulong copper mine) and Yunnan (*e.g.*, Bainiuchang polymetallic mine)

314   provinces/autonomous regions are the severe Mn pollution area. The hydrogeochemical cycling of

315   Fe and Mn in mining-affected aquatic systems is primarily governed by coupled geochemical

316   weathering processes and redox dynamics. Hydrodynamic conditions and water acidity play critical

317   roles in regulating the dissolution efficiency of these metals. It is well recognized that many metal

318   ores naturally contain Fe- and Mn-bearing minerals, which can release metal ions into solution

319   upon interaction with mine water, particularly under acidic conditions.

320   *3.2.4 Mining-affected water with high heavy metals*

321   For mining-affected waters characterized by elevated concentrations of HMs, including Cr,

322   Ni, Cu, Zn, As, Cd, Hg, and Pb, the identified spatial hotspots are largely consistent, mainly

distributed across the Yangtze River Basin as well as the provinces of Fujian, Gansu, Guangdong, and Guangxi (Figs. S8). These regions are well-known as major centers for non-ferrous metal production in China and play a critical role in the national mining industry (Zhang et al., 2016a). Notably, in the present study, the Baiyin copper mine in Gansu Province exhibits extreme levels of Cu, Zn, Cd, Hg, and Pb contamination. The Bainiuchang polymetallic mine, located in the southeastern Yunnan metallogenic belt, is identified as a significant source of Cr and As. In addition, the Zhongtiaoshan copper mining area is found to have the highest recorded concentration of Ni in AMD, reaching 15.0 mg/L.

In connection with the results summarized in Section 3.1, the top four HMs in acid water are Zn, Cu, Ni, and Pb, while that in non-acid water are Zn, Cu, Ni, and As. According to the review by Yin et al. (2018), the mineral composition of copper deposits is complex and includes associated minerals such as nickel, gold, and sulfur. Approximately 76% of the associated gold, 32.5% of the associated silver, and 76% of the sulfur originate from copper mines in China. This reason can explain the prevalence of Cu, Ni, and sulfate contamination hotspots in China's major copper production bases, *i.e.*, Jiangxi (Dexing/Yongping/Dongxiang, etc.), Tongling (Tongguanshan/Shizishan/Xinqiao, etc.), Daye (Tonglushan/Tongshankou, etc.), Zhongtiaoshan, Baiyin, and other copper bases (Chen et al., 2013). Besides, the Zn and Pb pollution levels are relatively higher in the Yunnan-Guizhou and Guangxi-Guangdong regions (Figs. S8d and S8h), where are abundantly occupied by the lead-zinc ores (*e.g.*, Dachang, Daxin, Wuxu, and Fankou lead-zinc mines, etc.). In these deposits, sphalerite (ZnS) and galena (PbS) are the principal mineral sources of Zn and Pb, respectively (Blowes et al., 2014). With respect to As contamination in mining-affected water, it has been demonstrated that pyrite (FeS_2) may contain substantial amounts

345 of As. Previous studies (Abraitis et al., 2004; Blanchard et al., 2007) have reported that As can

346 substitute for sulfur in the pyrite crystal lattice, forming As-S dianion groups. The incorporation of

347 As into pyrite enhances its chemical reactivity and accelerates its dissolution.

348 *3.3 Risks of mining-affected water in China*

349 Ingestion and dermal contact are the primary exposure pathways for both adults and children

350 residing in mining areas. The risks associated with such exposures are further exacerbated by the

351 persistence, mobility, and bioaccumulative potential of HMs in the environment. Among the metals

352 analyzed in this study, Cr, Ni, As, Cd, and Pb have been classified as carcinogenic to humans by

353 the International Agency for Research on Cancer. In this section, CRs are assessed specifically for

354 Cr, Cd, and As, as carcinogenic slope factors for the other metals are unavailable (Fig. 5).
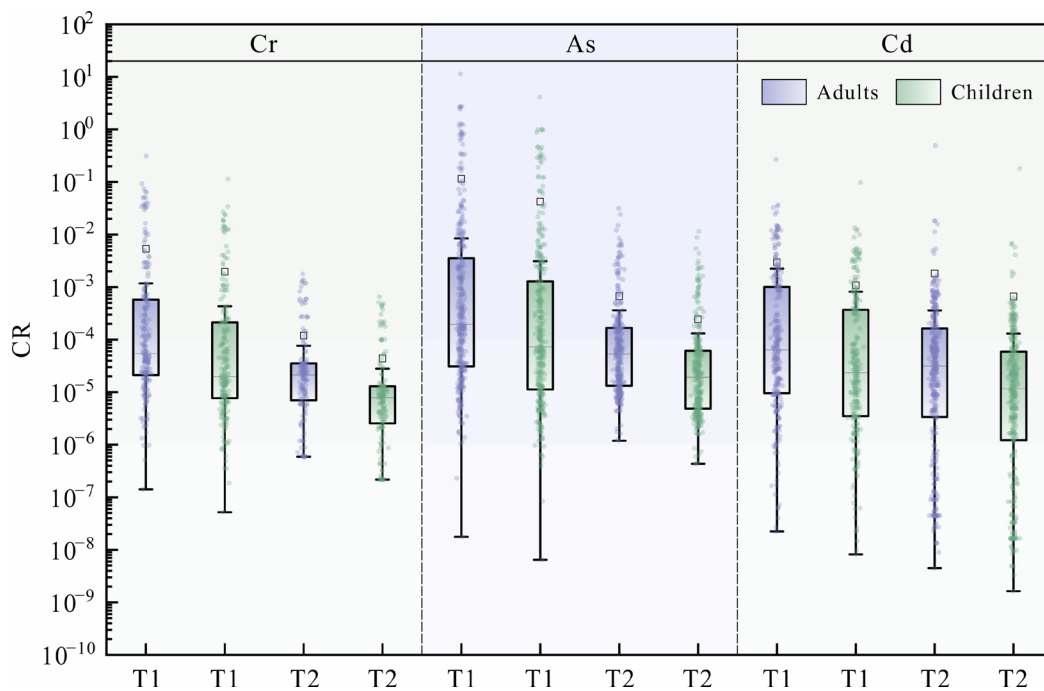
356 **Figure 5.** The CR value of Cr, As, and Cd in mining-affected water. T1 category includes mine

357 drainage, mine water, and leachate water, while T2 category indicates mining-affected surface

358 water and groundwater.

359   Additionally, Fe, Mn, Cr, Ni, Cu, Zn, As, Cd, and Pb are taken into consideration to calculate

360   the cumulative NCRs for residents (Fig. 6). To better illustrate the human health risks posed by

361   different types of mining-affected water in China, the risk assessment is categorized into two types:

362   T1 and T2. The T1 category includes mine drainage, mine water, and leachate water, which pose

363   significant threats to the surrounding water systems. The T2 category refers to surface water and

364   groundwater that have been affected by mining activities.

365
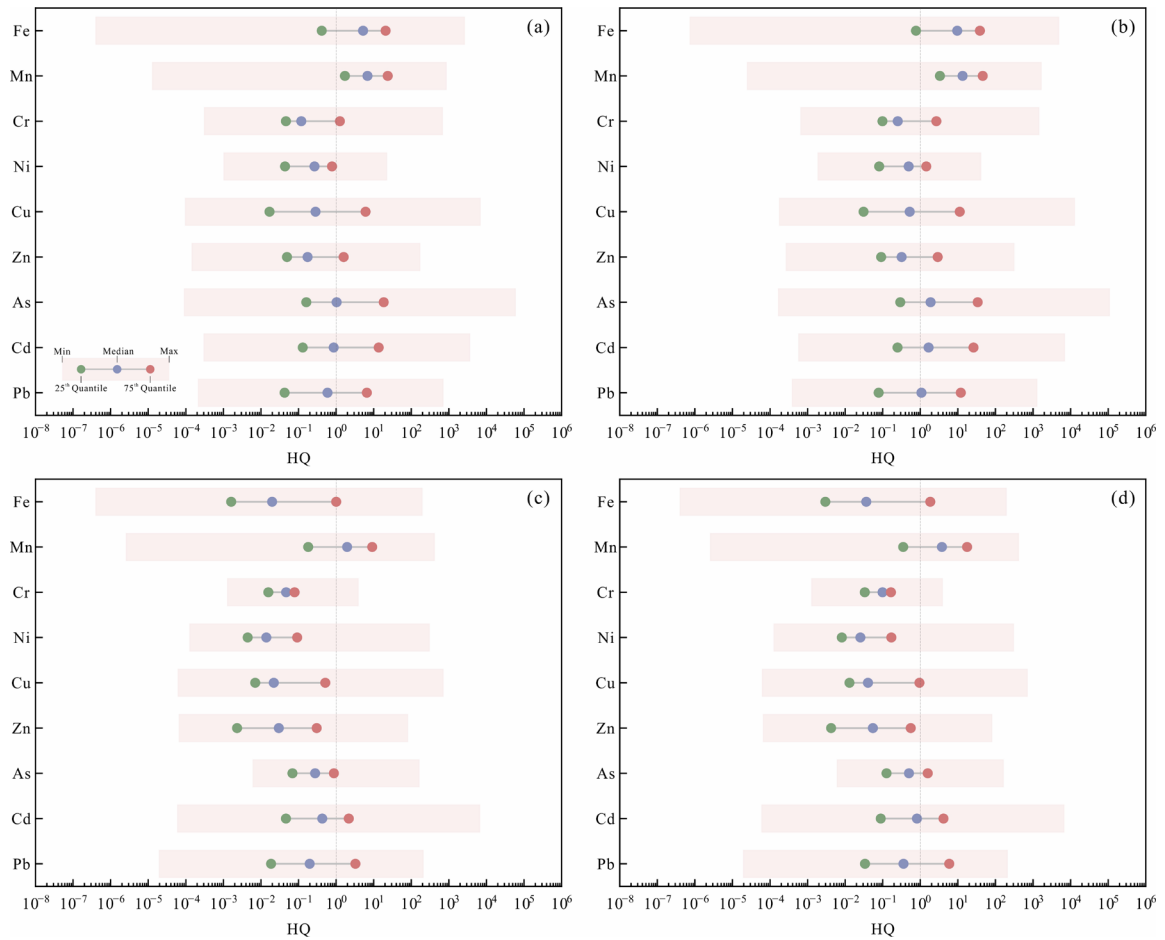
366   **Figure 6.** The HQ value of mining-affected water for (a) T1-Adult, (b) T1-Children, (c) T2-Adult,

367   and (d) T2-Children, respectively. T1 category includes mine drainage, mine water, and leachate

368   water, while T2 category indicates mining-affected surface water and groundwater.

369   *3.3.1 Carcinogenic risk of mining-affected water*

370   According to the guidelines established by the US EPA (2004), CR or TCR values in the range

371   of 10^{-6} to 10^{-4} are considered to be within the acceptable risk range. As shown in Fig. 5, the median

372   CR values for different population groups and water categories generally follow the order As > Cd >

373   Cr. This trend is consistent with the findings of Shi et al. (2018), who reported a similar risk ranking

374   for HMs in soils from mining areas. For T1-type water, the median CR values for all assessed

375   metals are below the upper limit of 10^{-4}, except for As exposure in adults. Specifically, the median

376   CR values for adults are As (1.98×10^{-4}) > Cd (6.40×10^{-5}) > Cr (5.39×10^{-5}), while for children

377   they are (7.24×10^{-5}) > Cd (2.34×10^{-5}) > Cr (1.97×10^{-5}). In comparison, the CR values associated

378   with T2-type water are generally lower than those for T1-type water. The median values for adults

379   are 5.28×10^{-5} (As), 3.14×10^{-5} (Cd), and 2.13×10^{-5} (Cr), while the corresponding values for

380   children are 1.93×10^{-5} (As), 1.15×10^{-5} (Cd), and 7.82×10^{-6} (Cr). Notably, the median TCR

381   values for both adults and children in the mining areas assessed in this study exceed the upper

382   acceptable limit, reaching 3.02×10^{-4} and 1.10×10^{-4}, respectively. In connection with the results

383   displayed in Fig. S9a, the mining areas with non-negligible CRs (TCR > 10^{-4}), primarily driven by

384   the combined effects of Cr, Cd, and As, account for 68.25 % of adults and 51.47% of children

385   exposed to T1-type water, and 40.27% of adults and 23.31% of children exposed to T2-type water.

386   In terms of spatial distribution (Fig. S10), the results indicate that TCR values associated with T1-

387   type water exceed the acceptable threshold in 55.00% (for adults) and 40.00% (for children) of the

388   mining areas. For T2-type water, the proportions of mining areas with unacceptable TCR values

389   are 51.52% (for adults) and 29.29% (for children). These results highlight the need for increased

390   attention and targeted management strategies in high-risk areas.

391 *3.3.2 Non-carcinogenic risk of mining-affected water*

392   For T1-type water (Figs. 6a and 6b) with high HQ values (HQ > 1), Mn, Fe, and As are

393 identified as the primary contributors to NCRs. The corresponding median HQ values for adults

394 are 6.84 (Mn), 5.21 (Fe), and 1.03 (As), while the values for children are 13.26 (Mn), 9.63 (Fe),

395 and 1.88 (As), respectively. In addition, for children, the median HQ values of Cd (1.66) and Pb

396 (1.07) also exceed the acceptable limit of 1. In the case of T2-type water (Figs. 6c and 6d), the

397 median HQ values for all assessed metals (except Mn) are below the USEPA threshold for both

398 adults and children. The descending order of median HQ values is as follows: Mn (1.950 for adults,

399 3.752 for children) > Cd (0.424, 0.812) > As (0.274, 0.500) > Pb (0.196, 0.357) > Cr (0.047, 0.099) >

400 Zn (0.030, 0.055) > Cu (0.022, 0.040) > Fe (0.020, 0.036) > Ni (0.014, 0.025). The results suggest

401 that children are more sensitive to the hazardous effects of HM exposure than adults, probably due

402 to the more conservative parameter settings used for children in the risk assessment model. In

403 connection with the results displayed in Fig. S9b, the mining areas with high HI values (HI > 1,

404 stemming from synergistic interactions among Fe, Mn, Cr, Ni, Cu, Zn, As, Cd, and Pb) account for

405 88.35 % (for adults) and 91.90% (for children) exposed to T1-type water. For T2-type water, the

406 corresponding proportions are 55.75% (for adults) and 63.10% (for children). As depicted in Fig.

407 S11, the southern regions are predominantly identified as NCR hotspots. Specifically, for T1-type

408 water, 89.04% (for adults) and 91.78% (for children) of mining areas exceed the acceptable HI

409 threshold, while in the case of T2-type water, the corresponding proportions are 68.07% and

410 80.67%, respectively.

4   Discussion

4.1   Underlying mechanisms of pronounced mining-affected water pollution in South China

The underlying mechanisms, including climatic conditions, geological factors, and mining practices, determine the spatial patterns of mining-affected water pollution in China, especially in the highly polluted southern regions. In terms of climatic conditions, the average temperature of the coldest month is > 0°C, while that of the hottest month is > 22°C, and the annual average precipitation is generally > 1,000 mm in South China. The high temperature and precipitation create a synergistic accelerator for mine water acidification. Elevated temperatures stimulate acidophilic microbial communities (*e.g.*, *Acidithiobacillus ferrooxidans*), which enhance enzymatic activity that catalyzes sulfide mineral oxidation. Combined with high levels of precipitation, rainfall infiltrates abandoned mines, tailings ponds, and exposed ore bodies, creating a sustained water-oxygen exchange that drives sulfuric acid formation and iron oxidation processes.

In terms of geological factors, the unique geo-environmental settings of South China, characterized by rugged topography, widespread sulfur-rich strata, and high background value of metallic minerals, result in mining-affected water with high acidity and elevated concentrations of sulfate, Fe, Mn, and HMs (Sun et al., 2022). The coal-forming periods of different mines in the South China coalfields are diverse, mainly Triassic, Neoproterozoic, etc., of which the sulfur enrichment exhibits strong links to marine-land interactions. The sustained seawater intrusion-regression cycle results in elevated sulfur contents (predominantly medium and high-sulfur coals) (Ai et al., 2023; Sun et al., 2025). As illustrated in Fig. S2, the coal fields in China exhibit sulfur contents ranging from 0.02% to 10.48%, with South China's coal-bearing areas showing the highest weighted average sulfur content (2.35%), including 29.63% of high-sulfur coal. Comparatively,

433   those weighted average sulfur contents of coal-bearing areas in Tibet-Western Yunnan, North China,

434   and Northeast China are 0.94%, 0.88%, and 0.86%, respectively (Tang et al., 2015). In addition, as

435   shown in Fig. S3, the metal mineral resources are abundant in the southern region of China, and

436   the water affected by mining practices is often highly toxic, with harmful HMs such as Cd, Pb, Hg,

437   Cr, As, Cu, and so on, endangering the surface water and groundwater systems (Sun et al., 2022).

438   As to mining practices, especially those involving sulfide-bearing metalliferous ore deposits

439   and sulfide-rich coal mining, are intrinsically associated with AMD. Acid drainage can occur

440   wherever sulfide minerals are excavated and exposed to atmospheric oxygen. The main sulfide

441   minerals in mine wastes are pyrite (FeS_2) and pyrrhotite ($Fe_{1-x}S$), while other associated sulfides

442   are prone to oxidation and release toxic elements, including Al, As, Cd, Co, Cu, Hg, Ni, Pb and Zn,

443   into the water flowing through the mine tailings (Blowes et al., 2014). The oxidation of FeS_2 by

444   atmospheric oxygen can be expressed by Eqs. (8) - (11). Moreover, underground mining is the

445   primary exploitation method in China. Substantial mined-out areas are formed after mining

446   activities, inducing the accumulation of groundwater and the formation of acid mine water. In

447   recent years, the phenomenon has intensified because a number of mines are abandoned without

448   proper closure measures (Jiang et al., 2020).

449    $$2FeS_2 + 7O_2 + 2H_2O \rightarrow 2Fe^{2+} + 4SO_4^{2-} + 4H^+ \tag{8}$$

450    $$4Fe^{2+} + O_2 + 4H^+ \rightarrow 4Fe^{3+} + 2H_2O \tag{9}$$

451    $$Fe^{3+} + 3H_2O \rightarrow Fe(OH)_3 + 3H^+ \tag{10}$$

452    $$FeS_2 + 14Fe^{3+} + 8H_2O \rightarrow 15Fe^{2+} + 2SO_4^{2-} + 16H^+ \tag{11}$$
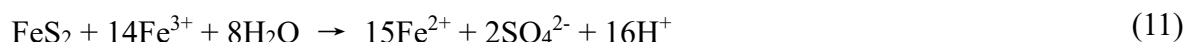
453   *4.2   Effects of mining-affected water pollution in China*

454   It is evident that acidic and metal-rich water is widespread in China, especially in the southern

areas (see Fig. 4 above and Fig. S8). As discussed in Section 4.1, the climatic conditions, geological

factors, and mining practices all play vital roles in the pronounced mining-affected water pollution

in South China. As a consequence, the contaminants pose significant risks to planetary health by

degrading surface water and groundwater quality, destroying biodiversity, and threatening human

well-being. Fig. 7 summarizes the key processes and adverse impacts of mining-affected water

pollution on the water subsystem, soil subsystem, and human health.
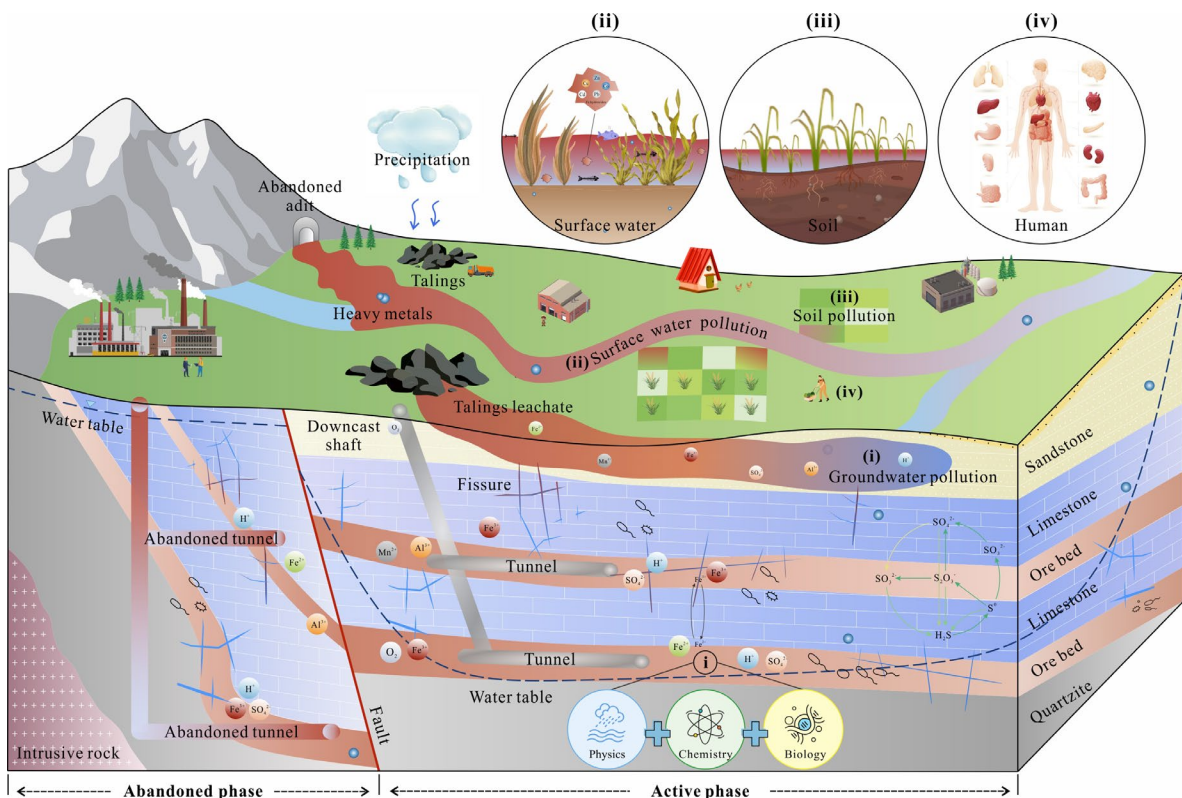
Figure 7. Conceptual model showing the processes and impacts of mining-affected water pollution

on (i) groundwater subsystem, (ii) surface water subsystem, (iii) soil subsystem, and (iv) human

health.

  ***Water subsystem*:** As a vital component of various ecosystems, the water environment faces

increasing challenges due to the presence of diverse mining-affected water pollution (as mentioned

in Section 3.2). On the one hand, mining activities can contaminate groundwater, making it unfit

for irrigation, drinking, and other purposes. In the active mining phase, the formation of AMD is

driven by coupled physical, chemical, and biological processes initiated through sulfide mineral oxidation in the presence of oxygen and water (Fig. 7). These interconnected reactions progressively degrade groundwater quality through acidification and contaminant mobilization (Acharya and Kharel, 2020); In terms of the abandoned phase, the weathering products of exposed sulfides can serve as a source of acidity, sulfate, and dissolved metals, which may subsequently migrate and transform within the recovering groundwater (Blowes et al., 2014). On the other hand, AMD from active and abandoned mines also contaminates water bodies, lowering pH levels and destroying habitats for fish and other aquatic organisms (Ighalo et al., 2021). Toxic metals have the potential to accumulate in the food chain, especially in aquatic organisms, making them one of the most severe contaminants in surface water. Moreover, given that the metals are difficult to biodegrade, their presence has led to detrimental effects on the ecological balance of aquatic ecosystems (Gu et al., 2014; Cui et al., 2021).

Soil subsystem: HMs can enter the soil through mining-affected water runoff and tailings leaching, which have been increasingly detected in soil environments worldwide. Excessive HMs disrupt soil physicochemical properties, impair soil organism viability through physiological dysfunction and behavioral inhibition, and diminish agricultural productivity. Furthermore, these contaminants induce structural shifts in microbial communities, reducing both the abundance and functional diversity of keystone microbial taxa essential for biogeochemical cycling. However, the adverse effects of mining-affected water pollution on the soil subsystem are not the focus of our study. This is because Shi et al. (2023) and Yu et al. (2024) have provided a more comprehensive analysis of the pollution status, risks, and major influencing factors in coal and metal mines across China.

Human health: The results of the human risk assessment presented in Section 3.3 highlight that the CRs and NCRs are severe in China. Moreover, the persistence, high mobility, and bioaccumulation potential of these metals in the environment substantially increase exposure risks, thereby amplifying their adverse health effects. The eight HMs examined in this study exhibit intrinsic toxicity, posing risks to human health through bioaccumulation pathways. Mechanistically, these HMs bind to DNA strands and enzyme-active sites, inducing disruptions in cellular homeostasis, endocrine signaling, immune responses, neurophysiological functions, and reproductive-endocrine systems (Shi et al., 2023; Meng et al., 2024). For example, various injuries linked to Cr exposure include nasal irritation and ulceration, skin irritation, and perforation of the eardrum. Acute exposure to Ni can result in damage to the kidneys, liver, and brain, whereas chronic exposure can cause tissue damage. Respiratory problems, dizziness, nausea, and diarrhea are common symptoms induced by elevated Cu concentrations (Gujre et al., 2021). Zn has a significant capacity for bioaccumulation, leading to increased health risks to the immune and nervous systems via the water-food chain (Cui et al., 2021). Chronic exposure to As is associated not only with skin lesions and skin cancer, but also with neurological, respiratory, cardiovascular, and developmental effects (Zhang et al., 2024). Poisoning with Cd can cause damage to the kidneys, bones, lungs, and liver, and can even lead to cancer. (Feng et al., 2022; Liu et al., 2024). Hg can lead to serious neurological disorders in both children and adults (Rui et al., 2017). Cardiovascular, central nervous system, kidney, and fertility problems are usually associated with Pb exposure (Shi et al., 2023). Furthermore, it has recently been demonstrated that Fe is linked to pathological disorders such as Alzheimer's and Parkinson's diseases (Sahoo and Sharma, 2023).

4.3   Implications for China's future differentiated management

In the mining areas, the rising HMs contamination and potential health risks in surface water and groundwater call for targeted and forward-looking control strategies in China. In fact, mining regulations differ across provinces and countries, highlighting the need for site-specific frameworks and criteria. Although management may vary by location, priorities must include land use history, mine type, available technology, eco-hydrological conditions, socio-economic factors, multi-stakeholder cooperation, long-term monitoring, effective enforcement of effluent limits, and treatment standards (Acharya and Kharel, 2020). Therefore, the differentiated management in the current study is an optimized regulatory paradigm that customizes strategies to mine types (coal vs. metal) and operational status (active vs. abandoned) based on hydrogeological conditions, pollution source characteristics, and multi-system sustainability requirements. The initiative aims to implement targeted intervention and precise prevention/control to mitigate pollution risks, restore and enhance ecological functions, while concurrently safeguarding human health.

Coal mine and metal mine: The results imply that the water pollution status in metal mines is higher than in coal mines (Figs. 3 and S5). To some extent, policymakers should enhance their focus on regulating metal mining water contamination and devise more effective measures to reduce exposure and manage risks. The results presented in Section 3.1 imply that the characteristic contaminants in the acid water of coal mines are sulfate (with a median of 1381.59 mg/L), Fe (77.41 mg/L), and Mn (3.50 mg/L), while that of metal mines also include a variety of HMs, such as Zn (7.20 mg/L), Cu (1.73 mg/L), Ni (0.21 mg/L), Pb (0.15 mg/L) and so on. Consequently, water quality monitoring frameworks and remediation technologies should adopt site-specific strategies to account for divergent pollutant profiles in metalliferous and coal mines. These customized

534   approaches should integrate contaminant sources, migration pathways, and ecotoxicological

535   impacts to ensure remediation effectiveness. Some studies have demonstrated that precipitation and

536   neutralization are commonly used methods in coal mines, while more complex technologies, such

537   as ion exchange or membrane separation techniques, are required to remove HMs in metal mines.

538   ***Active mine and abandoned mine***: The differentiated management policies for active and

539   abandoned mines aim to protect both the environment and public health across different stages of

540   mining operations. Active mining operations require AMD prevention frameworks focusing on

541   source control through sulfide oxidation suppression during the ore extraction and transport cycles.

542   This requires high-frequency sensor networks for real-time contaminant flux tracking and adaptive

543   mitigation protocols. In contrast, abandoned mine management prioritizes remediation-

544   performance validation, integrating long-term hydrogeochemical stability monitoring with

545   ecosystem resilience metrics. In addition, more scientific restoration strategies are critical to

546   rebuilding the sustainable development of the water subsystem and the soil subsystem disrupted by

547   legacy metal loads. Sustainable management also plays a pivotal role in addressing the challenges

548   of mining-related water pollution. Emphasis should be directed to multidisciplinary partnerships

549   and cost-effective and eco-friendly treatments, especially integrated treatment approaches that take

550   into account the synergy of source control and end-of-pipe treatment. These elements are crucial

551   for better understanding the complexities of mine drainage, controlling water quality degradation,

552   and minimizing socio-economic damage.

553   *4.4   Reliability, limitations and prospects*

554   To reveal the nationwide pollution status, spatial heterogeneity, health risks, and effects of

555   mining-affected water in China, a total of 8,433 water samples from 298 mines were integrated.

556   Additionally, the combination of data mining and quality assessment was employed to enhance the

557   reliability of the available data and build a high-quality database. However, there are still some

558   non-negligible limitations or uncertainties in the study.

559   On the one hand, the boundaries of mine sites are rarely clearly defined in the literature we

560   collected, which means that the spatial heterogeneity of mining-affected water pollution cannot be

561   accurately represented. On the other hand, the gridded data imply the southern regions, particularly

562   the provinces/autonomous regions of Guizhou, Guangdong, Fujian, Jiangxi, Hunan, and Guangxi,

563   are mining-affected water pollution hotspots. When compared with the reported sample sizes (Fig.

564   S4), this suggests that these areas are generally high-sampling zones, which may potentially distort

565   the representation of distribution. Therefore, it is of great importance to address the bias by (i)

566   combining the data mining and field sampling methods to investigate the potential contamination

567   levels in more coal and metal mines across China; (ii) balancing the sampling density within each

568   zone using bias correction techniques (*e.g.*, kernel density estimation and stratified spatial

569   resampling) to ensure the data representation; and (iii) incorporating spatial uncertainty into the

570   criteria to improve the spatial robustness for the assessments of mining-affected water pollution.

571   It is noteworthy that we cannot uncover the temporal evolution of mining-affected water

572   pollution due to the varying time scales of the data. Temporal variations in water chemistry (*e.g.*,

573   seasonal fluctuations and monsoon events) significantly impact the environmental fate of

574   contaminants and health risks through multiple mechanisms. During the monsoon season, heavy

575   rainfall flushes tailings ponds or open-pit mines, causing instantaneous spikes in HMs (*e.g.*, Cd, Cr,

576   and As) and sulfate concentrations. Meanwhile, the elevated groundwater levels associated with

577   high precipitation infiltration drive contaminant plumes along preferential pathways. These

dynamics introduce systematic biases into traditional static risk assessments. The annual or quarterly average risk assessment model may underestimate short-term high-dose exposure risks. Moreover, some gridded data only reflect the historical pollution status of a specific mine (*e.g.*, the Suichang gold mine and the coal mines in the Yudong River Basin) that has undergone successful ecological remediation and achieved good water quality levels after mining activities ceased.

Future in-depth research could focus on (i) gathering globally reported data through deep mining and quality control and establishing a high-quality global database to better understand the characteristics of mining-affected water pollution worldwide; (ii) identifying the key factors that govern the transport and transformation of contaminants in surface water and groundwater systems, during active and abandoned periods, and in coal and metal mines; (iii) enhancing the sustainable development of coal and metal mines by AI-driven digital simulations and digital twins, which can provide data-driven insights, optimize remediation endeavors, and advocate proactive measures to safeguard the environment; and (iv) strengthening the studies on the synergistic measures (not only at small-scale experimental sites but also at the mine site scale) to alleviate multifaceted environmental challenges in the mining-affected water and achieve the development of green mining.

5   Conclusions

In this study, the national status, spatial patterns, potential human health risks, and their multifaceted implications of mining-affected water pollution have been elucidated. The new and unique contributions of the current study are: (i) establishing a national-scale high-quality database covering 8,433 surface water or groundwater samples (6,175 coal mine water samples and 2,258 metal mine water samples) from 298 mines (211 coal mines and 87 metal mines) in 26

provinces/autonomous regions of China; and (ii) filling the gap of the nationwide spatial patterns of water pollution and associated health risks from both coal and metal mining activities for the first attempt. Specifically, eight heavy metals (i.e., Cr, Ni, Cu, Zn, As, Cd, Hg, and Pb) are considered in the current study. The main results are as follows:

- The predominant contaminants in both coal and metal mines in China are Zn, Ni and Cu. The detectable concentrations of several HMs are higher in most metal mines than in coal mines, especially in mining-affected water with low pH (< 6.5).

- The order of detectable median values of water affected by coal mining is Zn (0.4211) > Ni (0.1796) > Cu (0.0431) > Cr (0.0080) > Cd (0.0036) > As (0.0034) > Pb (0.0023) > Hg (0.0004), while that of water affected by metal mining is Zn (7.200) > Cu (1.7325) > Ni (0.2142) > Pb (0.1498) > Cr (0.0500) > Cd (0.0383) > As (0.0281) > Hg (0.0090).

- The pollution hotspots and potential risks of mining-affected water (with low pH, high sulfate, Fe, Mn, and HMs) are pronounced in the southern regions due to the synergistic mechanisms of climatic conditions, geological factors, and mining practices, especially in Guizhou, Guangdong, Fujian, Jiangxi, Hunan, and Guangxi provinces/autonomous regions.

- The unacceptable carcinogenic risks caused by poor-quality surface water and groundwater are observed in 51.52% (for adults) and 29.29% (for children) of the mining areas. Moreover, severe non-carcinogenic risks are also identified in 68.07% and 80.67% of mining areas for adults and children, respectively.

Accordingly, the findings of the study yield critical insights for designing differentiated management measures and formulating spatially-adaptive pollution control strategies across three key dimensions, including geographic scales (site-specific scale, provincial scale, or national scale),

mine types (coal or metal), and mining status (active or abandoned). This multidimensional

framework enables policymakers to strategically balance the trade-off between green mining

activities and human health priorities.

Data availability. The detailed data information can be found in Table S1.

Author contributions. ZYY, JS, JFW, and YY conceptualized the manuscript and its scope. ZYY, DGL, and YYS collected the data. ZYY prepared the initial manuscript with contributions from all co-authors. JS, JFW, YY, YYS, and JCW revised the manuscript.

Competing interests. The authors declare that they have no conflict of interest.

Financial support. This research is financially supported by the National Key Research and Development Program of China (2022YFC3702200), the China National Postdoctoral Program for Innovative Talents (BX20240165), the Jiangsu Funding Program for Excellent Postdoctoral Talents (2024ZB125), and the Fundamental Research Funds for the Central Universities (14380228).

References

Abraitis, P.K., Pattrick, R.A.D., and Vaughan, D.J.: Variations in the compositional, textural and electrical properties of natural pyrite: A review. Int. J. Miner. Process., 74, 41-59, https://doi.org/10.1016/j.minpro.2003.09.002, 2004.

Acharya, B.S. and Kharel, G.: Acid mine drainage from coal mining in the United States – An overview. J. Hydrol., 588, 125061, https://doi.org/10.1016/j.jhydrol.2020.125061, 2020.

Ai Y.L., Chen, H.P., Chen, M.F., Huang, Y., Han, Z.T., Liu, G., Gao, X.B., Yang, L.H., Zhang, W.Y., Jia, Y.F., and Li, J.: Characteristics and treatment technologies for acid mine drainage from

644 abandoned coal mines in major coal-producing countries. J. China Coal Soc., 48(12), 4521-

645 4535 (in Chinese with English abstract), https://doi.org/10.13225/j.cnki.jccs.2022.1846, 2023.

646 Blanchard, M., Alfredsson, M., Brodholt, J., Wright, K., Richard, C., and Catlow, A.: Arsenic

647 incorporation into FeS_2 pyrite and its influence on dissolution: A DFT study. Geochim

648 Cosmochim Acta, 71, 624-630, https://doi.org/10.1016/j.gca.2006.09.021, 2007.

649 Blowes, D.W., Ptacek, C.J., Jambor, J.L., Weisener, C.G., Paktunc, D., Gould W.D., and Johnson,

650 D.B. The geochemistry of acid mine drainage. Treatise on Geochemistry (Second Edition), 11,

651 131-190, https://doi.org/10.1016/B978-0-08-095975-7.00905-0, 2014.

652 Chen, D., Chen, Y.-P., and Lin, Y.: Heavy rainfall events following the dry season elevate metal

653 contamination in mining-impacted rivers: A case study of Wenyu River, Qinling, China. Arch.

654 Environ. Contam. Toxicol., 81, 335-345, https://doi.org/10.1007/s00244-021-00870-y, 2021.

655 Chen, J.P., Zhang, Y., Wang, J.X., Xiao, K.Y., Lou, D.B., Ding, J.H., Yin, J.N., and Xiang, J.: On

656 present situation and potential analysis of copper resources in China. J. Geol., 37, 358-365 (in

657 Chinese with English abstract), https://doi.org/10.3969/j.issn.1674-3636.2013.03.358, 2013.

658 Cheng, S.: Heavy metal pollution in China: origin, pattern and control. Environ. Sci. Pollut. Res.,

659 10(3), 192-198. https://doi.org/10.1065/espr2002.11.141.1, 2003.

660 Cui, L., Wang, X.N., Li, J., Gao, X.Y., Zhang, J.W., and Liu, Z.T.: Ecological and health risk

661 assessments and water quality criteria of heavy metals in the Haihe River. Environ. Pollut.,

662 290, 117971, https://doi.org/10.1016/j.envpol.2021.117971, 2021.

663 Dippong, T., Resz, M.-A., Tănăselia, C., and Cadar, O.: Assessing microbiological and heavy metal

664 pollution in surface waters associated with potential human health risk assessment at fish

665 ingestion exposure. J. Hazard. Mater., 476, 135187,

666 https://doi.org/10.1016/j.jhazmat.2024.135187, 2024.

667 Dong, F., Yin, H., Cheng, W., Li, Y., Qiu, M., Zhang, C., Tang, R., Xu, G., and Zhang, L.: Study on

668 water inrush pattern of Ordovician limestone in North China Coalfield based on

669 hydrochemical characteristics and evolution processes: A case study in Binhu and Wangchao

670 Coal Mine of Shandong Province, China. J. Clean. Product., 380, 134954,

671 https://doi.org/10.1016/j.jclepro.2022.134954, 2022.

672 Feng, Q., Li, T., Qian, B., Zhou, L., Gao, B., and Yuan, T.: Chemical Characteristics and Utilization

673 of Coal Mine Drainage in China. Mine Water Environ., 33, 276-286,

674 https://doi.org/10.1007/s10230-014-0271-y, 2014.

675 Feng, S., Deng, S., Tang, Y., Liu, Y., Yang, Y., Xu, S., Tang, P., Lu, Y., Duan, Y., Wei, J., Liang, G.,

676 Pu, Y., Chen, X., Shen, M., and Yang, F.: Microcystin-LR combined with cadmium exposures

677 and the risk of chronic kidney disease: a case-control study in central China. Environ. Sci.

678 Technol., 56 (22), 15818-15827, https://doi.org/10.1021/acs.est.2c02287, 2022.

679 Gu, D.Z., Li, J.F., Cao, Z.G., Wu, B.Y., Jiang, B.B., Yang, Y., Yang, J., Chen, Y.P.: Technology and

680 engineering development strategy of water protection and utilization of coal mine in China. J.

681 China Coal Soc., 46(10), 3079-3089 (in Chinese with English abstract),

682 https://doi.org/10.13225/j.cnki.jccs.2021.0917, 2021.

683 Gu, Y.G., Li, Q.S., Fang, J.H., He, B.Y., Fu, H.B., and Tong, Z.J.: Identification of heavy metals

684 sources in the reclaimed farmland soils of the pearl estuary in China using a multivariate

685 geostatistical approach. Ecotox. Environ. Saf., 105, 7-12,

686 https://doi.org/10.1016/j.ecoenv.2014.04.003, 2014.

Gujre, N., Rangan, L., and Mitra, S.: Occurrence, geochemical fraction, ecological and health risk assessment of cadmium, copper and nickel in soils contaminated with municipal solid wastes. Chemosphere, 271, 129573, https://doi.org/10.1016/j.chemosphere.2021.129573, 2021.

Gunson, A.J. and Jian, Y.: Artisanal mining in the People's Republic of China. International Institute of Environment and Development, 2001.

Havig, J.R., Grettenberger, C., and Hamilton, T.L.: Geochemistry and microbial community composition across a range of acid mine drainage impact and implications for the Neoarchean-Paleoproterozoic transition. J. Geophys. Res. Biogeosci., 122, 19, https://doi.org/10.1002/2016JG003594, 2017.

He, B., Yun, Z.J., Shi, J.B., and Jiang, G.B.: Research progress of heavy metal pollution in China: Sources, analytical methods, status, and toxicity. Chin. Sci. Bull., 58(2), 134-140, https://doi.org/10.1007/s11434-012-5541-0, 2013.

He, M., Wang, Z., and Tang, H.: The chemical, toxicological and ecological studies in assessing the heavy metal pollution in Le An River, China. Water Res., 32(2), 510-518, https://doi.org/10.1016/S0043-1354(97)00229-7, 1998.

Hou, Y., Zhao, Y., Lu, J., Wei, Q., Zang, L., and Zhao, X.: Environmental contamination and health risk assessment of potentially toxic trace metal elements in soils near gold mines – A global meta-analysis. Environ. Pollut., 330, 121803, https://doi.org/10.1016/j.envpol.2023.121803, 2023.

Hou, Z., Huang, L., Zhang, S., Han, X., Xu, J., and Li, Y.: Identification of groundwater hydrogeochemistry and the hydraulic connections of aquifers in a complex coal mine. J. Hydrol., 628, 130496, https://doi.org/10.1016/j.jhydrol.2023.130496, 2024.

709 Hu, H., Jin, Q., and Kavan, P.: A study of heavy metal pollution in China: Current status, pollution-

710   control policies and countermeasures. Sustainability, 6, 5820-5838,

711   https://doi.org/10.3390/su6095820, 2014.

712 Hu, R.Z., Liu, J.M., and Zhai, M.G.: Mineral resources science in China: a roadmap to 2050.

713   Science Press, Beijing, 2009.

714 Ighalo, J.O. and Adeniyi, A.G.: A comprehensive review of water quality monitoring and

715   assessment in Nigeria. Chemosphere 260, 127569,

716   https://doi.org/10.1016/j.chemosphere.2020.127569, 2020.

717 Ighalo, J.O., Kurniawan, S.B., Iwuozor, K.O., Aniagor, C.O., Ajala, O.J., Oba, S.N., Iwuchukwu,

718   F.U., Ahmadi, S., and Igwegbe, C.A.: A review of treatment technologies for the mitigation of

719   the toxic environmental effects of acid mine drainage (AMD). Process Safe. Environ. Protect.,

720   157, 37-58, https://doi.org/10.1016/j.psep.2021.11.008, 2022.

721 Jiang, C.F., Gao, X.B., Hou, B.J., Zhang, S.T., Zhang, J.Y., Li, C.C., and Wang, W.Z.: Occurrence

722   and environmental impact of coal mine goaf water in karst areas in China. J. Cleaner Product.,

723   275, 123813, https://doi.org/10.1016/j.jclepro.2020.123813, 2020.

724 Kumar, V., Paul, D., and Kumar, S.: Acid mine drainage from coal mines in the eastern Himalayan

725   sub-region: Hydrogeochemical processes, seasonal variations and insights from hydrogen and

726   oxygen stable isotopes. Environ. Res., 252, Part 4, 119086,

727   https://doi.org/10.1016/j.envres.2024.119086, 2024.

728 Li, Z., Ma, Z., van der Kuijp, T.J., Yuan, Z., and Huang, L.: A review of soil heavy metal pollution

729   from mines in China: Pollution and health risk assessment. Sci. Total Environ., 468-469, 843-

730   853, https://doi.org/10.1016/j.scitotenv.2013.08.090, 2014.

731   Liu, T., Yuan, X., Luo, K., Xie, C, and Zhou, L.: Molecular engineering of a new method for

732   effective removal of cadmium from water. Water Res., 253, 121326,

733   https://doi.org/10.1016/j.watres.2024.121326, 2024.

734   Liu, X., Shi, H., Bai, Z., Zhou, W., Liu, K., Wang, M., and He, Y.: Heavy metal concentrations of

735   soils near the large opencast coal mine pits in China. Chemosphere, 244, 125360,

736   https://doi.org/10.1016/j.chemosphere.2019.125360, 2020.

737   Ma, R., Gao, J., Guan, C., and Zhang, B.: Coal mine closure substantially increases terrestrial water

738   storage in China. Commun. Earth Environ., 5, 418, https://doi.org/10.1038/s43247-024-

739   01589-z, 2024.

740   Meng, F., Cao, R., Zhu, X., Zhang, Y., Liu, M., Wang, J., Chen, J., and Geng, N.: A nationwide

741   investigation on the characteristics and health risk of trace elements in surface water across

742   China. Water Res., 250, 121076, https://doi.org/10.1016/j.watres.2023.121076, 2024.

743   Moodley, I., Sheridan, C.M., Kappelmeyer, U., and Akcil, A.: Environmentally sustainable acid

744   mine drainage remediation: Research developments with a focus on waste/by-products. Miner.

745   Eng., 126, 207-220, https://doi.org/10.1016/j.mineng.2017.08.008, 2018.

746   Qu, S., Liang, X., Liao, F., Mao, H., Xiao, B., Duan, L., Shi, Z., Wang, G. and Yu, R.: Geochemical

747   fingerprint and spatial pattern of mine water quality in the Shaanxi-Inner Mongolia Coal Mine

748   Base, Northwest China. Sci. Total Environ., 854, 158812,

749   https://doi.org/10.1016/j.scitotenv.2022.158812, 2023.

750   Rui, L., Han, W., Jing, D., Fu, W., and Yi, L.: Mercury pollution in vegetables, grains and soils

751   from areas surrounding coal-fired power plants. Sci. Rep., 7, 1-9,

752   https://doi.org/10.1038/srep46545, 2017.

753 Sahoo, K. and Sharma, A.: Understanding the mechanistic roles of environmental heavy metal

754   stressors in regulating ferroptosis: adding new paradigms to the links with diseases. Apoptosis,

755   28(3), 277-292, https://doi.org/10.1007/s10495-022-01806-0, 2023.

756 Shi, J., Zhao, D., Ren, F., and Huang, L.: Spatiotemporal variation of soil heavy metals in China:

757   The pollution status and risk assessment. Sci. Total Environ., 871, 161768,

758   https://doi.org/10.1016/j.scitotenv.2023.161768, 2023.

759 Sun, J., Tang, C., Wu, P., Liu, C., and Zhang, R.: Migration of Cu, Zn, Cd and As in epikarst water

760   affected by acid mine drainage at a coalfield basin, Xingren, Southwest China. Environ. Earth

761   Sci., 69, 2623-2632, https://doi.org/10.1007/s12665-012-2083-3, 2013.

762 Sun, Y.J., Chen, G., Xu, Z.M., Yuan, H.Q., Zhang, Y.Z., Zhou, L.J., Wang, X., Zhang, C.H., and

763   Zheng, J.M.: Research progress of water environment, treatment and utilization in coal mining

764   areas of China. J. China Coal Soc., 45(1), 304-316 (in Chinese with English abstract),

765   https://doi.org/10.13225/j.cnki.jccs.YG19.1654, 2020.

766 Sun, Y.J., Guo, J., Xu, Z.M., Zhang, L., Chen, G., Xiong, X.F., Hua, J.F., Mu, L.J., and Wu, W.X.:

767   Spatial distribution characteristics of mine water quality in coal mining areas of China and

768   technological approaches for mine water treatment. J. China Coal Soc., 50(1), 584-599 (in

769   Chinese with English abstract), https://doi.org/10.13225/j.cnki.jccs.YG24.1547, 2025.

770 Sun, Y.J., Zhang, L., Xu, Z.M., Chen, G., Zhao, X.M., Li, X., Gao, Y.T., Zhang, S.G., and Zhu,

771   L.L.: Multi-field action mechanism and research progress of coal mine water quality

772   formation and evolution. J. China Coal Soc., 47(1), 423-437 (in Chinese with English abstract),

773   https://doi.org/10.13225/j.cnki.jccs.YG21.1937, 2022.

USEPA: Risk assessment guidance for superfund, Volume I: Human health evaluation manual final. U.S. Environment Protection Agency (Washington DC), 2004.

USEPA: Exposure factors handbook. U.S. Environment Protection Agency (Washington DC), 2011.

Wang, M., Wang, X., Zhou, S., Chen, Z., Chen, M., Feng, S., Li, J., Shu, W., and Cao, B.: Strong succession in prokaryotic association networks and community assembly mechanisms in an acid mine drainage-impacted riverine ecosystem. Water Res., 243, 120343, https://doi.org/10.1016/j.watres.2023.120343, 2023.

Wang, Y., Dong, R., Zhou, Y., and Luo, X.: Characteristics of groundwater discharge to river and related heavy metal transportation in a mountain mining area of Dabaoshan, Southern China. Sci. Total Environ., 679, 346-358, https://doi.org/10.1016/j.scitotenv.2019.04.273, 2019.

Wei, J., Hu, K., Xu, J., Liu, R., Gong, Z., and Cai, Y.: Determining heavy metal pollution in sediments from the largest impounded lake in the eastern route of China's South-to-North Water Diversion Project: Ecological risks, sources, and implications for lake management. Environ. Res., 24, 114118, https://doi.org/ 10.1016/j.envres.2022.114118, 2022.

Xiao, T., Boyle, D., Guha, J., Rouleau, A., Hong, Y., and Zheng, B.: Groundwater-related thallium transfer processes and their impacts on the ecosystem: southwest Guizhou Province, China. Appl. Geochem., 18(5), 675-691, https://doi.org/10.1016/S0883-2927(02)00154-3, 2003.

Yin, S., Wang, L., Kabwe, E., Chen, X., Yan, R., An, K., Zhang, L., and Wu, A.: Copper bioleaching in China: Review and prospect. Minerals, 8, 32, https://doi.org/10.3390/min8020032, 2018.

Yu, J., Liu, X., Yang, B., Li, X., Wang, P., Yuan, B., Wang, M., Liang, T., Shi, P., Li, R., Cheng, H., and Li, F.: Major influencing factors identification and probabilistic health risk assessment of soil potentially toxic elements pollution in coal and metal mines across China: A systematic

796   review. Ecotoxicol. Environ. Saf., 274, 116231, https://doi.org/10.1016/j.ecoenv.2024.116231,

797   2024.

798 Zhang, L.-Z., Xing, S.-P., Huang, F.-Y., Xiu, W., Rensing, C., Zhao, Y., and Guo, H.M.: Metabolic

799   coupling of arsenic, carbon, nitrogen, and sulfur in high arsenic geothermal groundwater:

800   Evidence from molecular mechanisms to community ecology. Water Res., 249, 120953,

801   https://doi.org/10.1016/j.watres.2023.120953, 2024.

802 Zhang, M.C., Chao, L.J., Yuan, L.P., Liang, W.J., Zheng, X., and Sun, K.F.: Summarize on the lead

803   and zinc ore resources of the world and China. China Mining Mag., 25, 41-45 (in Chinese

804   with English abstract), 2016a.

805 Zhang, X., Li, X., and Gao, X.: Hydrochemistry and coal mining activity induced karst water

806   quality degradation in the Niangziguan karst water system, China. Environ. Sci. Pollut. Res.,

807   23, 6286-6299, https://doi.org/10.1007/s11356-015-5838-z, 2016b.